

## Effect of Metal Foam's Volume on the Performance of a Double Pipe heat exchanger

Zuhair S. Faal<sup>1</sup>, Abbas J. Jubear<sup>1</sup>, Hussain R. Al-Bugharbee<sup>1</sup>

### Affiliations

<sup>1</sup>Mechanical Engineering Department, Wasit University, Wasit, Iraq.

### Correspondence

Zuhair S. Faal  
[zuhairsa302@uowasit.edu.iq](mailto:zuhairsa302@uowasit.edu.iq)

### Received

06-November-2023

### Revised

16-December-2023

### Accepted

17-January-2024

### Doi:

[10.31185/ejuow.Vol12.Iss2.495](https://doi.org/10.31185/ejuow.Vol12.Iss2.495)

### Abstract

The present numerical study aims to explore the effect of the metal foam's volume on the performance of a double-pipe heat exchanger in comparison with a double-pipe heat exchanger with a smooth pipe (HXS). Water was used as an operating fluid at flow rate 2Lpm. The outer stainless steel pipe has an outer diameter ( $D_o=60\text{mm}$ ) and length ( $L=609.6\text{mm}$ ), and an inner copper pipe with an outer diameter ( $d_o=20\text{mm}$ ). The numerical simulation was conducted by employing ANSYS FLUENT 2020 R2 software. The open-cell copper foam (CF) with the porosity of (0.9) was used. The cases considered in the analysis including a heat exchanger with a complete fill of copper foam (HXF), and a partial fill heat exchanger. The latter was made by inserting a complete rings of copper foam baffles (CFB) to decrease volume of a CF. Then, the baffles volumes increased by increasing the thickness and number of baffles. Three parameters were varied then their influence on performance evaluate criteria (PEC) were investigated. The parameters were pore density (PPI), thickness of baffles ( $t_c$ ), and number of baffles ( $nob$ ). Results showed that, heat transfer rate ( $Q_{ave}$ ) and the pressure drop ( $\Delta p$ ) increased with the increase of pore density, where the ( $Q_{ave}$ ) reached to (17%) at pore density (10-50PPI) in (HXF), and well distribution of a CFB could increase the thermal performance while the pressure drop did not change with use the same volume of the CF.

**Keywords:** performance evaluate criteria; metal foam baffles; copper foam; heat transfer enhancement

**الخلاصة:** تهدف الدراسة العددية الحالية إلى استكشاف تأثير حجم الرغوة المعدنية على أداء مبادل حراري ثنائي الأنابيب مقارنة بمبادل حراري ثنائي الأنابيب خالي من الرغوة المعدنية أو امس الانبوب (HXS). إنها تستخدم الماء كسائل تشغيل بمعدل تدفق 2 لتر في الدقيقة، الأنابيب الخارجي المصنوع من الفولاذ المقاوم للصدأ له قطر خارجي ( $D_o=60\text{mm}$ ) وطول ( $L=609.6\text{mm}$ )، وأنبوب نحاسي داخلي بقطر خارجي ( $d_o=20\text{mm}$ ). تم إجراء المحاكاة العددية بواسطة برنامج ANSYS FLUENT 2020 R2 وتم استخدام رغوة النحاس ذات الخلية المفتوحة (CF) ذات مسامية مقدارها (0.9). تشمل الحالات التي تم النظر فيها في التحليل، مبادل حراري مملوء بالكامل برغوة النحاس (HXF)، ومبادل حراري مملوء جزئياً. تم تصنيع هذا الأخير عن طريق إدخال حلقات كاملة من حواجز الرغوة النحاسية (CFB) لتقليل حجم الرغوة النحاسية. ومن ثم تم زيادة حجم الحواجز بزيادة سمكها وعددها. تم تغيير ثلاث معلمات وتم دراسة تأثيرها على معايير تقييم الأداء (PEC). وهي كثافة المسام (PPI)، وسمك الحواجز ( $t_c$ )، وعدد الحواجز ( $nob$ ). أظهرت النتائج أن كلا من معدل انتقال الحرارة ( $Q_{ave}$ ) وانخفاض الضغط ( $\Delta p$ ) يزدادوا مع زيادة كثافة المسامية، حيث ان معدل انتقال الحرار يصل الى (17%) عند كثافة المسام (10-50 PPI) في المبادل الحراري المملوء (HXF). والتوزيع الجيد لحواجز الرغوة المعدنية يزيد من الأداء الحراري بينما لم يتغير انخفاض الضغط مع استخدام نفس الحجم من الرغوة النحاسية.

Nomenclature			
$a_{sf}$	Solid-fluid specific surface area ( $\text{m}^2$ )	$T_{ci}, T_{co}$	Inlet and outlet cold water temperature ( $^{\circ}\text{C}$ )
$A_i, A_o$	Inner and outer Surface area of inner pipe ( $\text{m}^2$ )	$T_{hi}, T_{ho}$	Inlet and outlet hot water temperature ( $^{\circ}\text{C}$ )
$A_c$	Cross section area of annular gap ( $\text{m}^2$ )	<b>Greek Symbols</b>	
$d_i, d_o$	Inner and outer diameter of inner pipe (m)	$\rho$	Density ( $\text{kg}/\text{m}^3$ )
$D_i, D_o$	Inner and outer diameter of outer pipe (m)	$\mu$	Viscosity ( $\text{N}\cdot\text{s}/\text{m}^2$ )
$D_a$	Darcy Number	$\Delta p$	Pressure drop across the heat exchanger (Pa)
$d_f$	Fiber diameter (mm)	$\epsilon$	Porosity of the porous medium
$d_p$	Pore diameter (mm)	$p$	Wetted perimeter (m)
$F$	Inertial coefficient of metal foam	<b>Subscript</b>	

$h_{sf}$	Solid-fluid interfacial specific heat transfer coefficient ( $Wm^{-2} \text{ } ^\circ K^{-1}$ )	$i, o$	Inlet and outlet
$f_{MF}$	Friction factor with metal foam	$h, c$	Hot and cold
$f_s$	Friction factor without metal foam (smooth)	$ave$	Average
$k_{fe}$	Effective thermal conductivity of fluid ( $W/m \cdot k$ )	$s$	Surface
$k_{se}$	Effective thermal conductivity of solid ( $W/m \cdot k$ )	<b>Abbreviations</b>	
$k_p$	Effective thermal conductivity in metal foam ( $W/m \cdot k$ )	tc	thickness of baffles
$k$	Permeability of the porous medium (m)	nob	number of baffles
$K$	Thermal conductivity ( $W/m \cdot k$ )	HXS	double-pipe heat exchanger with a smooth pipe
$Nu_{MF}$	Nusselt number with metal foam	HXF	double-pipe heat exchanger with full foam
$Nu_s$	Nusselt number without metal foam (smooth)	HX109	double-pipe heat exchanger with (tc=10 & nob=9)
$p_{c,i}, p_{c,o}$	Inlet and Outlet pressure for the outer pipe (pa)	HX209	double-pipe heat exchanger with (tc=20 & nob=9)
$P_r$	Prantel Number	HX1018	double-pipe heat exchanger with (tc=10 & nob=18)
$R_e$	Renault Number	CF	copper foam
$T_f, T_s$	Temperature of fluid and the solid matrix ( $^\circ K$ )	CFB	copper foam baffles
$T_{s1}, T_{s2}$	Surface temperature on the inner pipe ( $^\circ C$ )	PEC	performance evaluate criteria

## 1. INTRODUCTION

More industries today require heat exchangers have small size and high performance. There are several ways to enhance the performance. The ways can include using rough and extended surfaces, and porous media. Therefore, using open cell metal foam to increase surface area to transfer heat has been an important way. Metal foams have good characteristics including high compressive strength, lightweight, stiff, ability to be formed into complex shapes with void spaces making up 75–95% of the volume, low relative density, high thermal conductivity of the cell edges, large accessible surface area per unit volume, and the ability to mix fluid.

In Abadi & Kim, 2017 [1], a narrow (4mm diameter) copper tube was filled with copper foams of 20 and 30PPI. It was experimentally examined in a heat exchanger arrangement. Working fluid was R245fa refrigerant, the pressure drop with the heat transfer coefficient are compared with an empty tube. Experiments show that reducing the cross sectional area of the channel made most predictive methods unable of predicting the experimental results. This was explained by the imperfections of the metal foam mesh caused by the foam sheets being cut into small cylinders. Compared to most of the predictions, damaged ligaments, damaged pores, and fewer pores in the cross sectional area result in a lower pressure drop and heat transfer coefficient.

Xu et al., 2018 [2], examined numerically fully developed forced convective heat transfer in tubes soldered with novel porous structures (Gradient metal foam GMF) that were partially filled. The pore densities of gradient metal foams are less than 40 PPI and the porosities exceed 0.8. Brinkman extended Darcy model and two equation model adjusting for a LTNE effect are employed for energy equations. The results are shown that the friction factor reduces with rising porosity over the whole porosity area.

A computational analysis on a counter-flow double pipe heat exchanger operating in turbulent flow with two configurations was carried out by Jamarani et al., 2017 [3], Copper porous media considered with porosity of (0.9). When the porous media was put in the centre of the inner pipe and on the inner surface of the outer pipe, the non-dimensional thickness of the porous material that offered the best thermal performance was ( $S=0.7$ ). However, with the configuration, which the porous material was fixed at the inner and outer surfaces of the inner pipe, ( $S=0.4$ ) was the optimum non-dimensional thickness.

Fiedler et al., 2021 [4], investigated the effectiveness of a novel alloy of metal foam ZA27 with a heat exchanger. Through a casting technique, open cell metal foam was bonded with a pipe. Foam's macroscopic density was (1.28–1.36g/cm<sup>3</sup>) and an interconnected porosity was (72–74 vol.%). The temperature difference was about 42 kelvin. The results showed an increase in heat transfer of up to 71%. However, overall performance was found to be constrained by poor heat transfer between copper tube and internal mass stream, as a result of the relatively small contact surface.

Tamkhade et al., 2023 [5], the evaluation of performance to a double-pipe heat exchanger with an inner tube made of stainless steel, and an outer tube made of galvanized iron was investigated numerically by using CFD analysis. With hot water (80°C) and 2 LPM in the inner tube and cold water (30°C) and 10 Lpm in the outer tube as the working fluids, nickel metal foam with pore densities (10 to 50PPI) and 0.9 porosity is used. The results are shown that heat transfer coefficient of stream through an annular flow passage with the metal foam and overall heat transfer coefficient increased together with the rise in the pore density.

Li et al., 2020 [6] studied a triple-tube latent heat storage system with nanoparticles and metal foam with porosities (0.95, 0.97, 0.99) to solve a problem of phase change materials' low thermal conductivity. While water transfers heat through the inner and outer tubes. The effects of using metal foam and nanoparticles alone and together were investigated. The results showed that by decreasing the metal foam's porosity reduce the time needed for melting and solidification, where was at metal foam of 95% porosity without nanoparticles, the time reduce by 83.7% and 88.2%, respectively, compared with the pure system.

In Chen et al., 2020 [7], an novel shell-and-tube heat exchanger with baffle metal foam (5, 10, 20 and 40PPI) with porosity (0.9118- 0.9520), was utilized to recover heat from exhaust gas. Thermal hydraulic performance to metal foam baffle in heat exchanger systems was investigated using a three-dimensional numerical model, the metal foam baffle heat exchangers with (40PPI) and Porosity (0.9132) prove the best performance results, and the overall performance of heat exchangers with metal foam baffles increases as the thickness of the metal foam increases.

In a different research, Zhou et al., 2021 [8], studied metal foam-wrapped cylinders in a shell and tube condenser during sloshing conditions such as surging, swaying, heaving, rolling, pitching, and yawing. The sloshing frequency varied from 0 to 0.33 Hz, and the sloshing angle ranges from 0° to 12°, open-cell copper foams with pore densities of (5, 10, 20, and 40PPI) were brazed to a copper tube. The highest performance for condensation heat transfer in heat exchanger with 10PPI copper foam, was 34% -54% larger than heat exchanger without metal foam.

A detailed examination to using different size of metal foam baffles in double pipe heat exchangers and its effect on their thermal and hydraulic performance was presented in the current study. The influence of baffles thickness, their number, and pore density, as well as their distribution were also examined.

The purpose of the current study improving the heat transfer rate in double pipe heat exchanger, because of its impact on many thermal devices. Heat energy may be transferred between two fluids at different temperatures using double-pipe heat exchangers. It is utilized in several industrial processes, refrigeration devices, cooling technologies, applications for sustainable energy, and other fields. Double pipe heat exchangers are categorized differently into cross, counter, and parallel flows in all utilized it.

## 2. NUMERICAL SIMULATION

ANSYS 2020 R2, was used to conduct solution and complete mathematical representation of the physical problem including continuity equation and momentum equation as well as energy equation.

### 2.1. Mathematical Model

#### 2.1.1. Geometry

Figure (1) shows the details of drawing of the physical geometry model for a double pipe heat exchanger. All dimensions were quoted from Ebieto et al., 2020 [1] after validated it. The stainless steel outer pipe has a 609.6mm length, outer diameter ( $D_o$  60mm) with (1.5mm) thickness and it was insulated from outer with two copper caps (10mm) thickness. And copper inner pipe was with length 711.2mm, outer diameter ( $d_o$  20mm) and (1mm) thickness. Metal foam was open-cell and has porosity (0.9) and pore density was change as (10, 20, 30, 40 and 50PPI). Annular gap of heat exchanger is completely filled with metal foam at the first step to give heat exchanger with full foam (HXF), after that it is partially filled with rings baffles with thickness ( $t_c=10$ mm) and number of baffles ( $nob=9$ ), and denoted it as (HX109). Then, volume of CF was gradually increased by used two method. First, by changing the thickness to ( $t_c=20$ mm) with the same ( $nob$ ) to get (HX209) and the second was by changing the number of baffle ( $nob=18$ ) with keeping the same thickness ( $t_c=10$ ) to get (HX1018). Thus, there are five main configurations of heat exchangers namely HXF HX109, HX209, and HX1018 and smooth pipe heat exchanger (HXS), as shown in Figure (2).

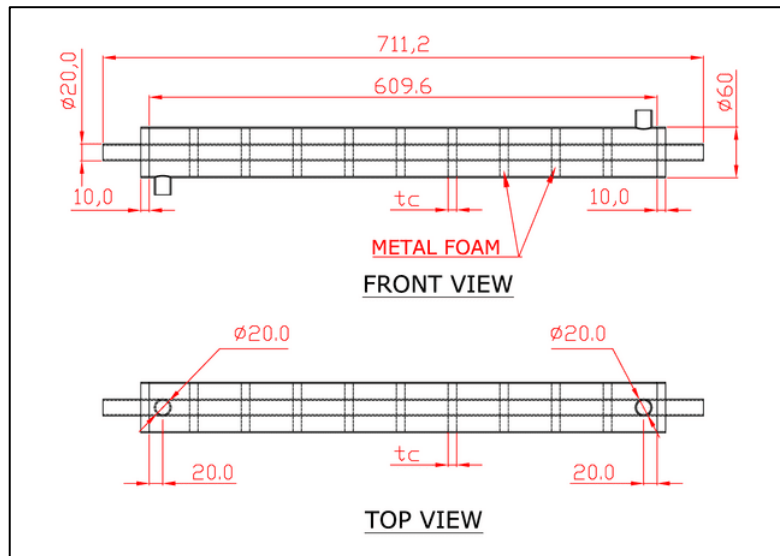


Figure 1 Details drawing of the physical model geometry dimensions in mm.

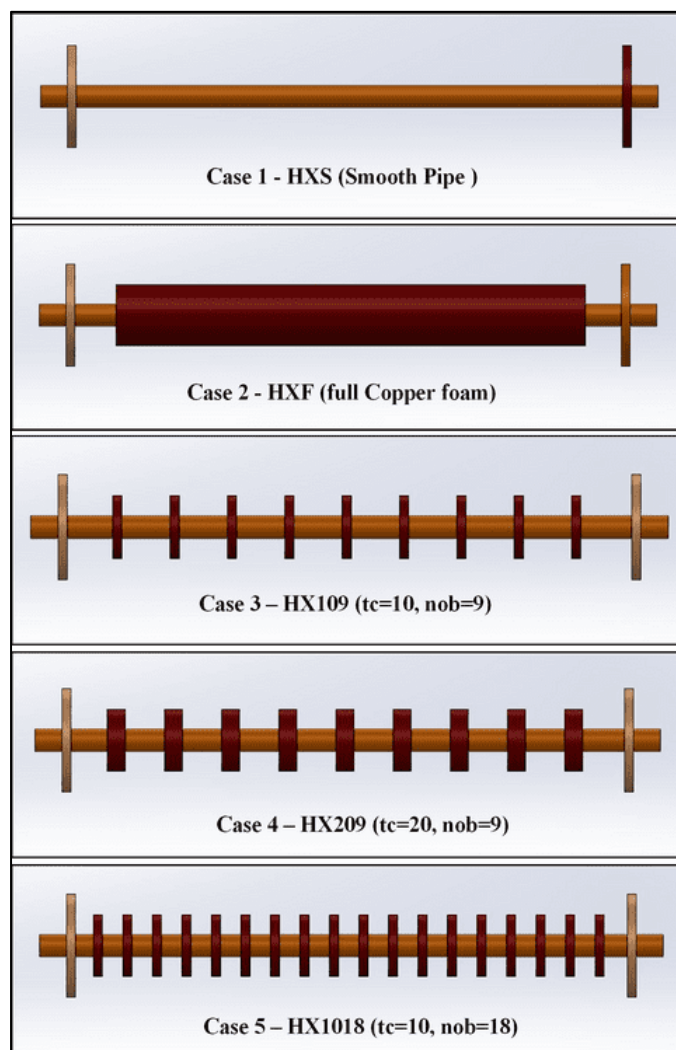


Figure 2 Descriptions of the studied cases

## 2.1.2. Mathematical Assumptions

The descriptive analysis is based on the following simplifying assumptions: -

- 1- Steady state conditions.
- 2- Simulation with three dimensional (x, y, z).
- 3- Thermophysical properties are constant in solid or fluid phases.
- 4- Isotropic, rigid, uniform and homogeneous metal foam
- 5- Fouling is neglected.
- 6- Heat generation and viscous dissipation are neglected.
- 7- Flow is turbulent.
- 8- A local thermal non-equilibrium (LTNE) model is used with equations of energy.

## 2.1.3. Governing Equations

To analyze fluid flow and heat transfer, the governing differential equations are presented. The fluid region's waterflow field is described by the Navier-Stokes equation, while the flow field inside an isotropic homogeneous porous medium is presented in a volume-averaged generalized momentum equation which described by the Brinkman-Forchheimer extended Darcy model. These equations will be presented in the following sections.

### 2.1.3.1. Conservation of Mass

Any closed system's mass is constant and does not fluctuate over time according to the laws of mass conservation [9].

$$\frac{\partial V_x}{\partial x} + \frac{\partial V_y}{\partial y} + \frac{\partial V_z}{\partial z} = 0 \quad (1)$$

### 2.1.3.2. Momentum equations

The change rate in momentums equal to the net forces that acting on a bodies according to Navier-Stokes equations and Newton's second law of motion [10] is:

**In X-direction**

$$\frac{1}{\varepsilon^2} (V_x \frac{\partial V_x}{\partial x} + V_y \frac{\partial V_x}{\partial y} + V_z \frac{\partial V_x}{\partial z}) = -\frac{\partial p}{\partial x} + \frac{1}{\varepsilon Re} \left( \frac{\partial^2 V_x}{\partial x^2} + \frac{\partial^2 V_x}{\partial y^2} + \frac{\partial^2 V_x}{\partial z^2} \right) - \frac{1}{Da Re} V_x - \frac{F}{\sqrt{Da}} V_x |\vec{V}| \quad (2)$$

**In Y-direction**

$$\frac{1}{\varepsilon^2} (V_x \frac{\partial V_y}{\partial x} + V_y \frac{\partial V_y}{\partial y} + V_z \frac{\partial V_y}{\partial z}) = -\frac{\partial p}{\partial y} + \frac{1}{\varepsilon Re} \left( \frac{\partial^2 V_y}{\partial x^2} + \frac{\partial^2 V_y}{\partial y^2} + \frac{\partial^2 V_y}{\partial z^2} \right) - \frac{1}{Da Re} V_y - \frac{F}{\sqrt{Da}} V_y |\vec{V}| \quad (3)$$

**In Z-direction**

$$\frac{1}{\varepsilon^2} (V_x \frac{\partial V_z}{\partial x} + V_y \frac{\partial V_z}{\partial y} + V_z \frac{\partial V_z}{\partial z}) = -\frac{\partial p}{\partial z} + \frac{1}{\varepsilon Re} \left( \frac{\partial^2 V_z}{\partial x^2} + \frac{\partial^2 V_z}{\partial y^2} + \frac{\partial^2 V_z}{\partial z^2} \right) - \frac{1}{Da Re} V_z - \frac{F}{\sqrt{Da}} V_z |\vec{V}| \quad (4)$$

Energy equation of the fluid in the porous medium (LTNE) is:

$$(V_x \frac{\partial T_f}{\partial x} + V_y \frac{\partial T_f}{\partial y} + V_z \frac{\partial T_f}{\partial z}) = \frac{(1+k_f)}{Pr Re} \left( \frac{\partial^2 T_f}{\partial y^2} + \frac{\partial^2 T_f}{\partial z^2} \right) + \frac{h_{sf} a_{sf}}{K_{sf} Pr Re} (T_s - T_f) \quad (5)$$

Energy equation of the solid matrix (LTNE) is:

$$0 = \frac{\partial^2 T_s}{\partial y^2} + \frac{\partial^2 T_s}{\partial z^2} + \frac{h_{sf} a_{sf}}{K_{se}} (T_f - T_s) \quad (6)$$

The equation of energy for an incompressible fluid can be written in a form as a thermal equation for static temperature (without foam) is:

$$(\mathbf{u} \cdot \nabla)T = \alpha \nabla \cdot (\nabla T) \tag{7}$$

## 2.2. Numerical model

Governing equations must be solve through Finite volume method to modelling heat transfer and fluid flow in simple and collector geometric shapes through uses a computer code package, that are hard to solve in other programming languages.

### 2.2.1. Geometry creation

The annular model with and without metal foam is drawn by using (SolidWorks2022) software program. The model was imported to the geometry in (Ansys fluent 2020 R2).

### 2.2.2. Meshing the geometry

An acceptable mesh is used to arrive at the optimal converged solution. Hexahedron and Tetrahedron mesh technology were used for the model geometry's 3-D mesh, as shown in Figure (3). Using (inflation) and (sizing) to regulate the shape of the mesh specially with copper foam parts give more accurate values of temperature, the number of elements was (4,400,000 to 4,700,000). This range was varied depending on the studied cases.

#### 2.2.2.1. Mesh independency

To verify mesh dependence, a reduced size of the element should be made. Figure (3) shows that the element size was taken as (1.3mm) to get the best mesh, the accuracy and resolution must be adopted in a comparison of solutions by average Nusselt number for various mesh models. Depending on the cases that were analyzed, the number of pieces ranged from 3,400,000 to 4,700,000.

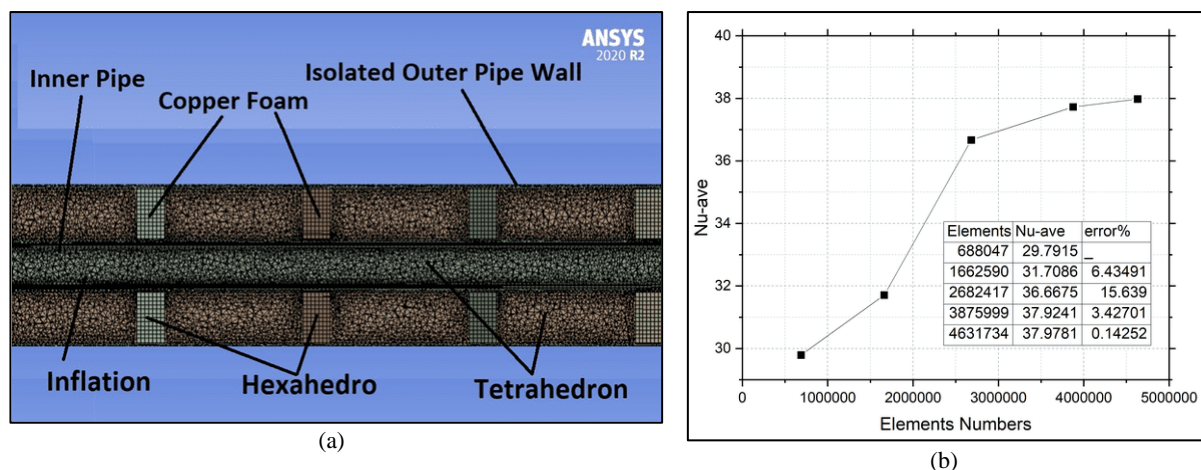


Figure 3 (a) Grid generated for Present model (b) Mesh independency.

### 2.2.3. Numerical setup

#### 2.2.3.1. General setting and models

Four processes parallel and double precision solver were selected, atmospheric pressure, steady-state time, absolute velocity are considered. The gravity (-g) in (Y) direction, simulation of the buoyancy model is carried out. Type of governing models (energy, viscous) are selected with activating on the energy equation. The k-ε realizable model is suitable [11], it is chosen too.

#### 2.2.3.2. Setting boundary conditions

The present study is taken inlet temperatures as (75°C and 30°C) for hot and cold water at inlet and (2 lpm) as flow rate with insulated outer pipe. The main parameters which taken is showed in Table (1) and Figure (5) to explain the boundary conditions of inlet laminar flow.

**Table 1** Boundary conditions.

Zone	Type	Momentum B.C.	Thermal B.C
cold-inlet	mass-flow-inlet	- Gage Pressure=0 Pa. - Reference: Absolute - Method: Normal to Boundary	Temperature
hot-inlet	mass-flow-inlet	- Gage Pressure=0 Pa. - Reference: Absolute - Method: Normal to Boundary	Temperature
cold-outlet hot-outlet	outflow	-	-
wall-outer-pipe	wall	Stationary, No slip	Insulated No heat flux
wall-inner-pipe	wall	Stationary, No slip	via system coupling

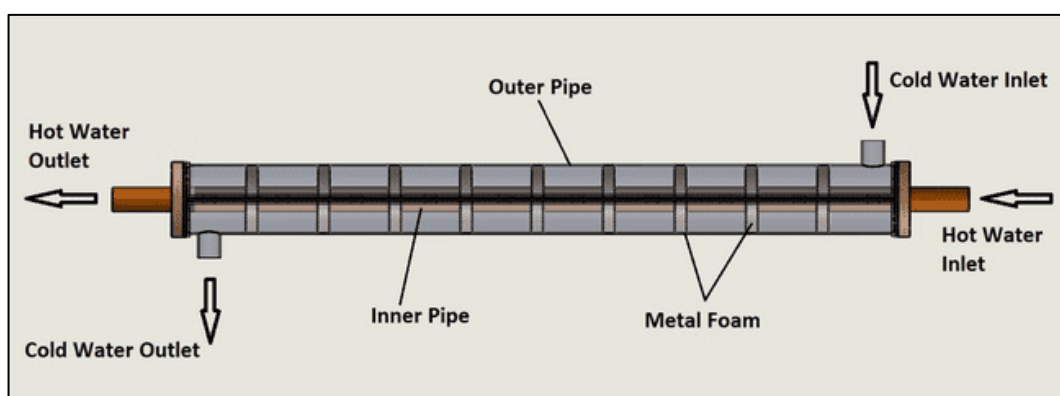


**Figure 5** Boundary conditions of geometrical model

### 2.2.3.3. Operating conditions

For the present work, the gravity = - 9.81 in Y-direction and temperature ambient as operating temperature and the operating pressure selected is 101.325 kPa.

### 2.2.3.4. Convergence criterion

Using a set of residual values below, the solver checks for convergence of the solution using the residuals technique, and stops when the average residuals decrease. "Residuals" are the inaccuracy in the computation. It is authorized if the flow residuals, comprising the continuity and momentum characteristics, are less than  $10^{-4}$  and  $10^{-5}$ . As seen in Figure (6), the convergence criterion was taken as  $10^{-6}$  for the pressure residual, and  $10^{-3}$  for all of the other residuals [11]. Whereas, the time spent varied depending on the case from one hour to three hours.

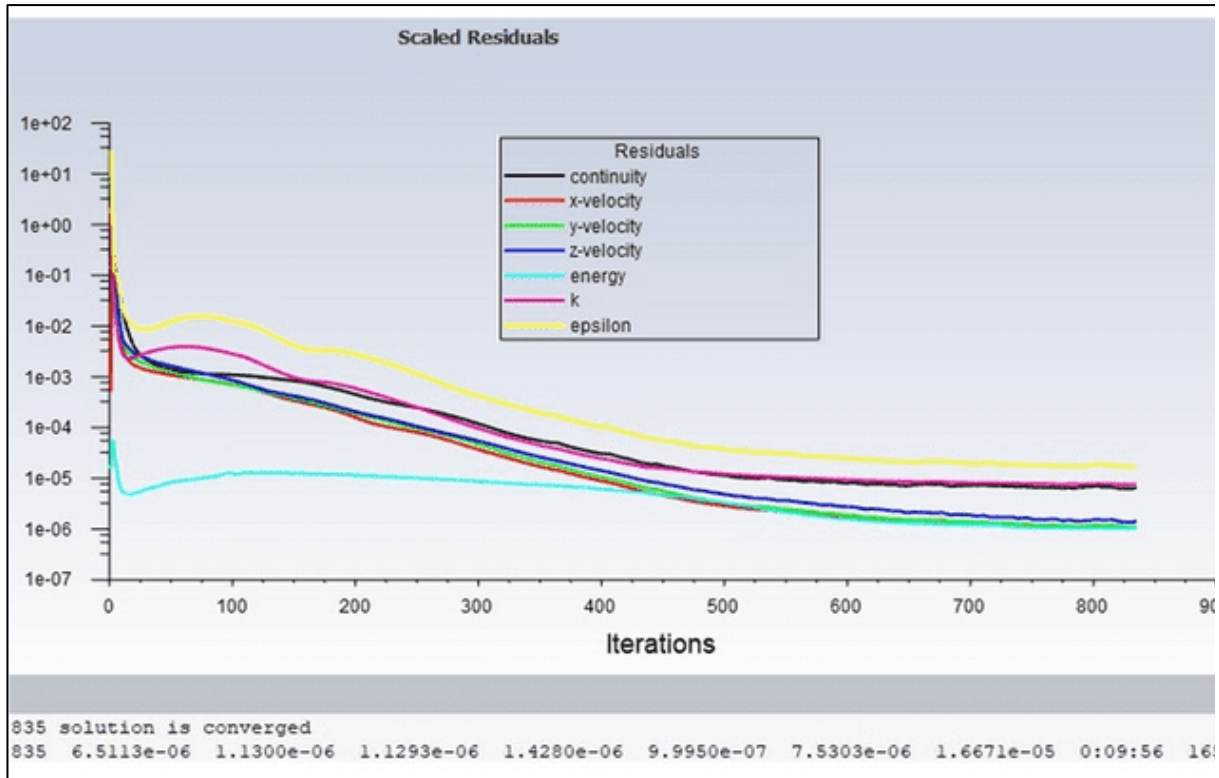


Figure 6 Variation of Numerical Residuals with Iteration.

Four surface temperature on the inner pipe, which were ( $T_{S1}$ ,  $T_{S2}$ ,  $T_{S3}$ , and  $T_{S4}$ ), inlet and outlet temperature for both pipes ( $T_{hi}$ ,  $T_{ho}$ ,  $T_{ci}$ , and  $T_{co}$ ), and inlet with outlet pressure for outer pipe ( $p_{ci}$  and  $p_{co}$ ), were set as shown in Figure (7).

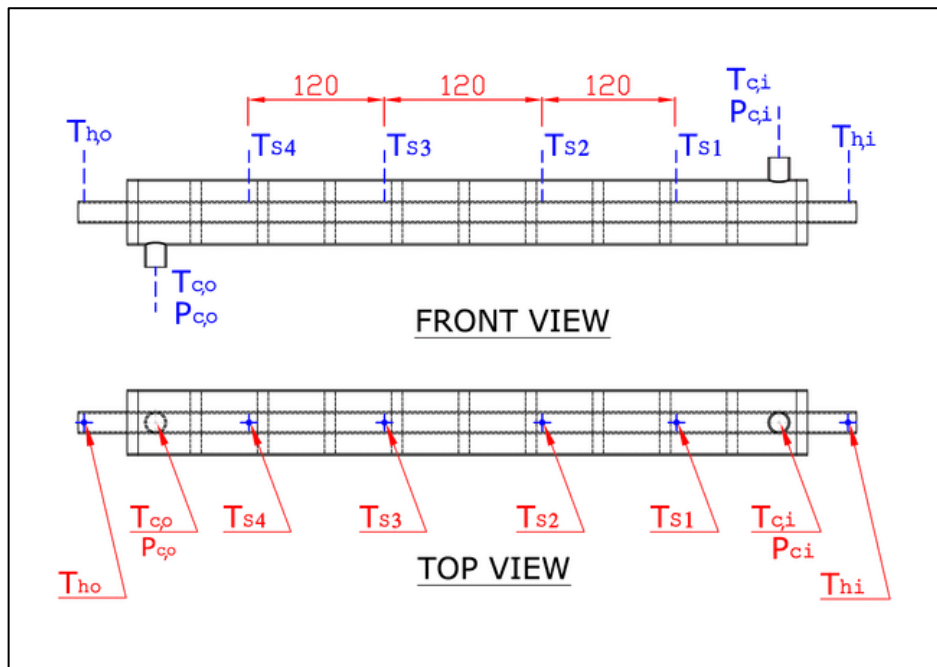


Figure 7 The geometrical model with four surface temperature.

### 3. CALCULATIONS

In order to finalize the mathematical representation of the physical problem, some partial differential equations, such as Equations (8-21), need to be resolved as follows:

#### 3.1. Calculation of Thermal performance

- The heat transfer rate calculations from the hot water to the cold water is calculated according to the following procedure [12]:

Heat transfer of the hot water ( $Q_h$ ) is :

$$Q_h = (\dot{m}C_p)_h (T_{h,i} - T_{h,o}) \quad (\text{W}) \quad (8)$$

Heat transfer to cold water ( $Q_c$ ) is :

$$Q_c = (\dot{m}C_p)_c (T_{c,o} - T_{c,i}) \quad (\text{W}) \quad (9)$$

- The average heat transfer rate ( $Q_{ave}$ ) between the hot water and cold water side is :

$$Q_{ave} = \frac{Q_h + Q_c}{2} \quad (\text{W}) \quad (10)$$

- The maximum heat transfer ( $Q_{max}$ ) can be given as :

$$Q_{max} = (\dot{m}C_p)_h (T_{h,i} - T_{c,i}) \quad (\text{W}) \quad (11)$$

- The effectiveness of the double pipe heat exchanger (E) is obtained from :

$$E = \frac{Q_{ave}}{Q_{max}} \quad (12)$$

- The convection heat transfer coefficient ( $h_i$ ) between the hot water and Inner surface of the copper pipe:

$$h_i = \frac{Q_{ave}}{A_i(T_{h,ave} - T_{s,ave})} \quad (\text{W/m}^2 \cdot ^\circ\text{C}) \quad (13)$$

- The log mean temperature difference ( $\Delta T_{LM}$ ) for parallel flow is:

$$\Delta T_{LM} = \frac{(T_{h,i} - T_{c,i}) - (T_{h,o} - T_{c,o})}{\ln[(T_{h,i} - T_{c,i}) / (T_{h,o} - T_{c,o})]} \quad (^\circ\text{C}) \quad (14)$$

- The overall heat transfer coefficient ( $U_i$ ) is:

$$U_i = \frac{Q_{ave}}{A_i \Delta T_{LM}} \quad (\text{W/m}^2 \cdot ^\circ\text{C}) \quad (15)$$

- The outer convection heat transfer coefficient of cold water ( $h_o$ ) is:

$$h_o = \frac{1}{A_o \left( \frac{1}{U_i A_i} - \frac{1}{h_i A_i} - \frac{\ln\left(\frac{d_o}{d_i}\right)}{2\pi KL} \right)} \quad (\text{W/m}^2 \cdot ^\circ\text{C}) \quad (16)$$

- The hydraulic diameter ( $D_h$ ):

$$D_h = \frac{4A_c}{p}, \quad A_c = \left(\frac{\pi}{4}\right)(D_i^2 - d_o^2)$$

$$D_h = \frac{4A_c}{p} = \frac{4 \times \left(\frac{\pi}{4}\right)(D_i^2 - d_o^2)}{\pi D_i + \pi d_o} = D_i - d_o \quad (\text{m}) \quad (17)$$

Where  $p$  : Wetted perimeter (m)

- The average Nussle number ( $Nu_{ave}$ ) on the outer surface of the inner cylinder can be expressed as follows:

$$Nu_{ave} = \frac{h_o D_h}{K_f} \quad (18)$$

### 3.2. calculation of Hydraulic Performance

- The velocity ( $u$ ) was estimated using the following equation [13]:

$$u = \frac{\dot{V}}{A_c} = \frac{4\dot{V}}{\pi(D_i^2 - d_o^2)} \quad (\text{m/s}) \tag{19}$$

- The friction factor ( $f$ ) is calculated for the cold stream from using the following :

$$f = \frac{\Delta P \left(\frac{D_h}{L}\right)}{\frac{\rho u^2}{2}} \tag{20}$$

Where  $\Delta P$  : Pressure drop (pa)

### 3.3. Calculation of Performance evaluate criteria (PEC)

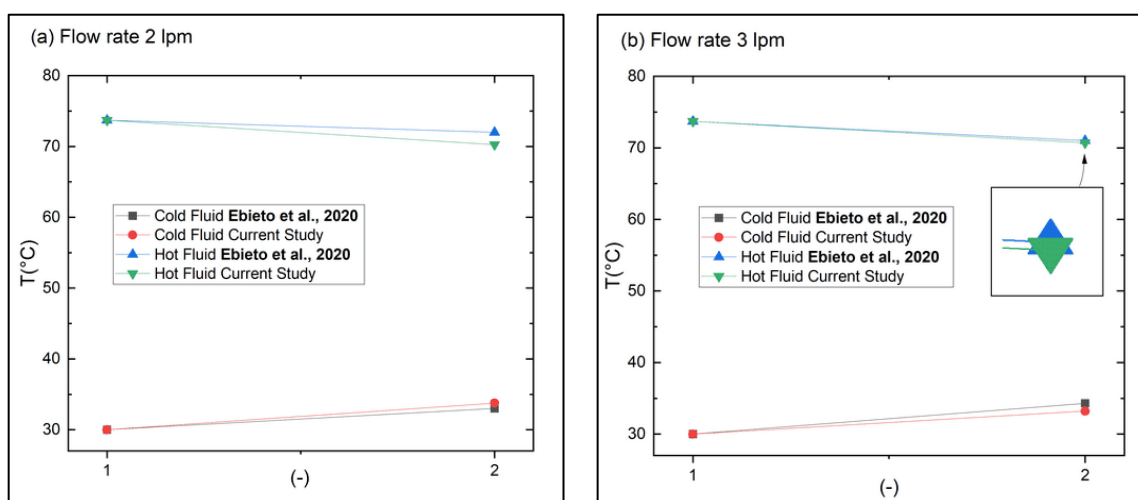
- The performance evaluate criteria of the double-pipe heat exchanger (PEC) for cold water side is :

$$PEC = \frac{\left(\frac{Nu_{MF}}{Nu_s}\right)}{\left(\frac{f_{MF}}{f_s}\right)^{\frac{1}{3}}} \tag{21}$$

## 4. RESULTS AND DISCUSSIONS

### 4.1. Validation of Experimental heat exchanger

It is necessary to firstly validate experimental model for a HXS in order to know accuracy of simulation software (Ansys 2020 R2). Then, its dimensions to make 3D drawing of double pipe heat exchanger with metal foam which can be in the simulation of the current study. Ebieto et al., 2020 [1], has been select to this validation when change water temperature with floe rate (2, 3, and 4LPM) in parallel flow, and the deviation was (2.3%, 2%, and 1.8%) respectively as showed in Figure (8). This small percentage of deviation explains the accuracy of the simulation software in that the practical results closely approximate the theory. Since the research presented by Ebieto et al., 2020 is experimental research, therefore can be used the simulation software in the current study to extract theoretical results.



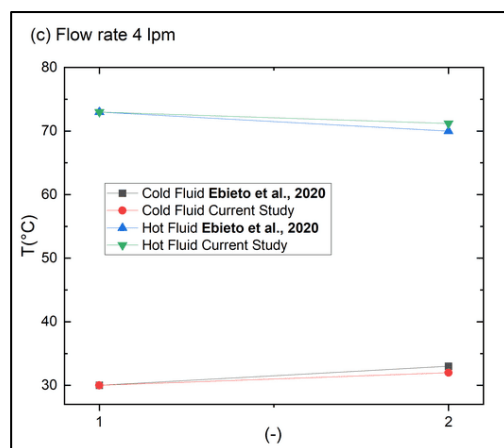


Figure 8 Validation of a smooth pipe heat exchanger.

## 4.2. Numerical Results

Effect of three parameters pore density (PPI), thickness of baffle foam ( $t_c$ ), and number of baffles foam ( $nob$ ) on thermal performance which include heat transfer rate ( $Q_{ave}$ ), Nusselt number ( $Nu_{ave}$ ) and the effectiveness ( $E$ ) were obtained. Hydraulic performance which included the pressure drop ( $\Delta p$ ) and the friction factor ( $f$ ), then performance evaluate criteria (PEC) have been explored to four heat exchangers with copper foam, additionally to HXS as showed in Figure (2).

### 4.2.1. Thermal performance

#### 4.2.1.1. Effect pore density (PPI)

In Figure (9), pore density of copper foam has been changed as (10, 20, 30, 40, and 50 PPI) to four heat exchangers (HXF, HX109, HX209, and HX1018), and explained its effect on thermal performance, as it has been observed in Figure (9 a) that heat transfer rate ( $Q_{ave}$ ) increases gradually with the increase in pore density, and the effect of this increasing less with increases pore density after (40PPI). Same behavior noted in Figure (9 b, c) with other factors of thermal performance, Nusselt number ( $Nu_{ave}$ ) and the effectiveness ( $E$ ). Where  $Nu$  and  $E$  increase with Pore density increasing, attributed this improvement to increase surface area of metal foam with increase pore density.

#### 4.2.1.2. Effect thickness of baffles foam ( $t_c$ ) and Number of baffles foam

In Figure (9), the effect of copper foam volume and its distribution has been studied as well by using the parameters, thickness of baffle foam and Number of baffles to give three type different heat exchangers (HX109, HX209, and HX1018), where same volume have been used in (HX209 and HX1018) with different distribution. It was observed that, when the volume of metal foam decrease all parameters (i.e.  $Q_{ave}$ ,  $Nu_{ave}$ , and  $E$ ) decrease. In addition, it was noted that when same volume of copper foam is used, but with different distribution, those parameters ( $Q_{ave}$ ,  $Nu_{ave}$ , and  $E$ ) in a (HX1018) becomes better than in (HX209). This means there are possibly to improve thermal performance without increase the volume. The reason for this behavior can be attributed to the fact that increasing number of baffles ( $nob$ ) while decreasing their thickness ( $t_c$ ) leads to increase surface area of CFB and an increase in mixing and turbulence flow as well, which reduces the boundary layers.

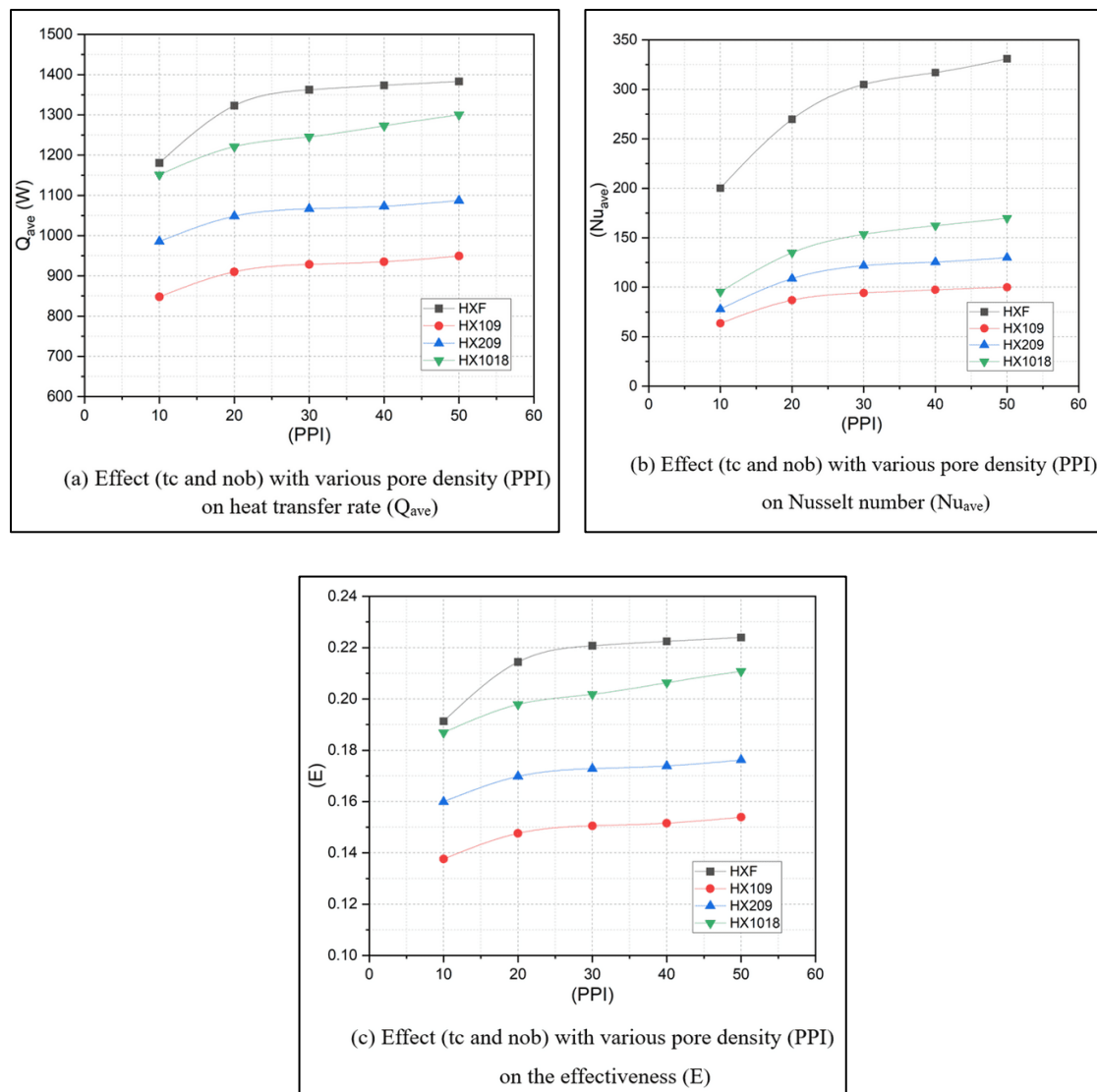


Figure 9 Effect of parameters (PPI, tc, nob ) on thermal performance.

## 4.2.2. Hydraulic performance

### 4.2.2.1. Effect Pore density (PPI)

In Figure (10), same parameter was change, pore density (10, 20, 30, 40, and 50 PPI) to briefly describe its effect on hydraulic performance for (HXF, HX109, HX209, and HX1018), as it has been observed there is a penalty for improvement thermal performance due to increase both the pressure drop ( $\Delta p$ ) and the friction factor ( $f$ ) with increase pore density (PPI). The reason of that is attributed to the increase of struts of cells with increases pore density that cause increase the friction through obstruct flow water.

### 4.2.2.2. Effect thickness of baffles foam (tc) and Number of baffles foam

In Figure (10), effect of CFB volume and its distribution has been studied to the three heat exchangers (HX109, HX209, and HX1018) on hydraulic performance as well. It was observed that, when decreases the volume of CFB, both parameters ( $\Delta p$  and  $f$ ) decrease. Furthermore, when same volume of CFB are used but with different distribution in both (HX209 and HX1018), the pressure drop and the friction factor remain constant. This means there is not a possibility to decrease penalty through increase or decrease number of baffles if it was complete ring.

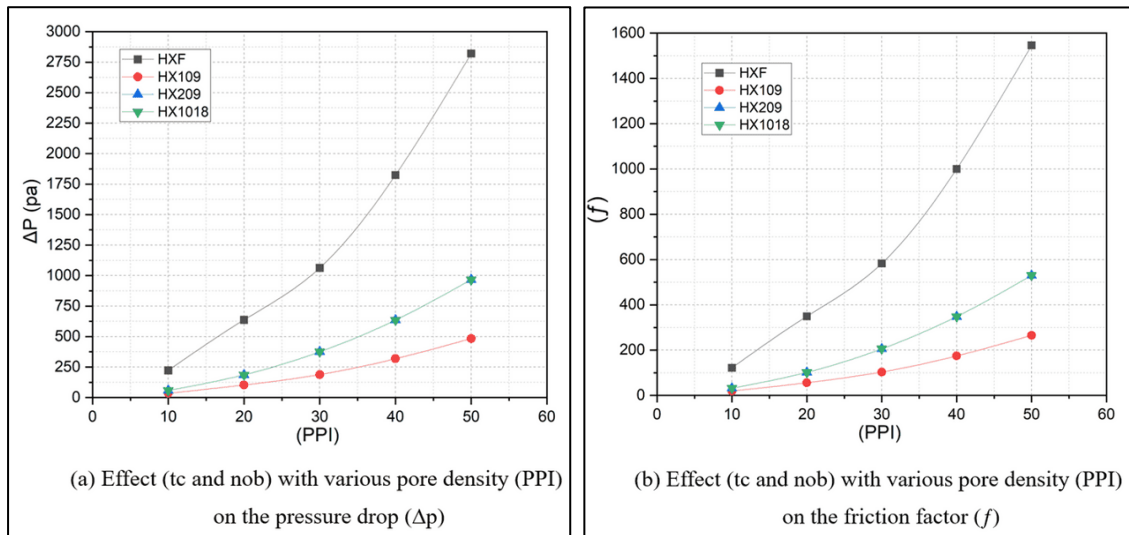


Figure 10 Effect of parameters (PPI, tc, nob ) on hydraulic performance

### 4.2.3. Performance evaluate criteria (PEC)

Comparison has been made between improvement in thermal performance and penalty in pressure drop and friction factor through calculate performance evaluate criteria (PEC).

#### 4.2.3.1. Effect Pore density (PPI) , thickness of baffle (tc), and Number of baffles (nob)

Figure (11), showed that PEC of four heat exchangers (HXF, HX109, HX209, and HX1018) has a gradual decreasing when increases pore density and volume of copper foam. It is noted that PEC of HXF at (40 and 50PPI) is close to PEC of HX1018 at (10 and 20PPI). This means that PEC can be improved by decreasing the volume and pore density to reach what heat exchanger with full foam has reached with bigger pore density. It was also observed that when using the same volume of metal foam with a HX209 and HX1018, there will be a clear difference in PEC where HX1018 has greater value. That means it can improve PEC through found better distribution to metal foam with use the same volume.

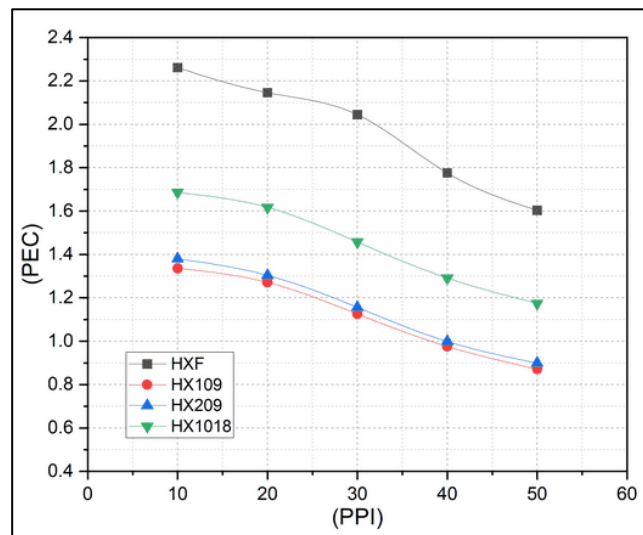


Figure 11 Effect (tc and nob) with various pore density (PPI) on performance evaluate criteria (PEC)

### 4.3. Comparison of contours shapes

A comparison of contour shapes, which belong to three heat exchangers (HXS, HXF, and HX1018), are shown in Figure (12) at plane (X=58.8cm) which explains a side section at exit of fluid and front section in Figure (13). It was observed that the bluish color was in largest area in a HXS, where the area decreased in a HX1018, and area was least in a HXF, it explains that the largest heat transfer convection occurs in the HXF. Moreover, the reddish color to hot fluid in the inner pipe was the largest gradient in a HXS and very weakly in the HXF.

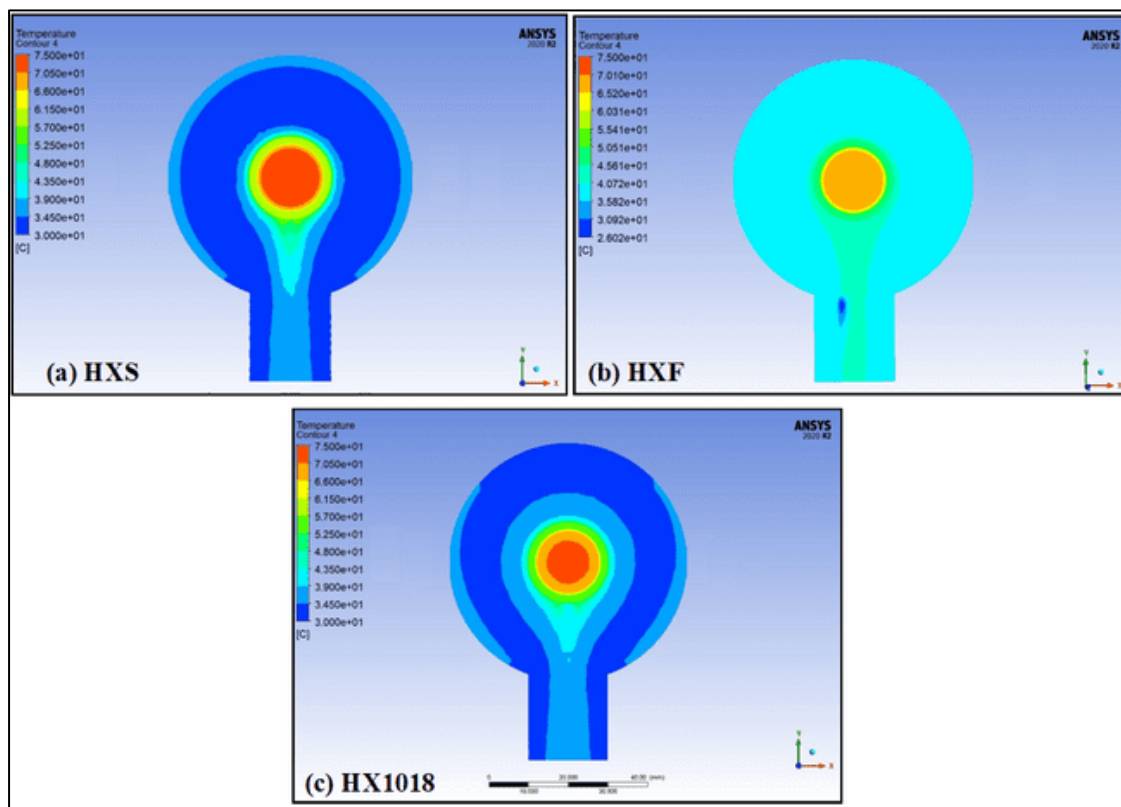


Figure 12 Contour of temperature at (X=58.8mm) for a three heat exchangers (side view).

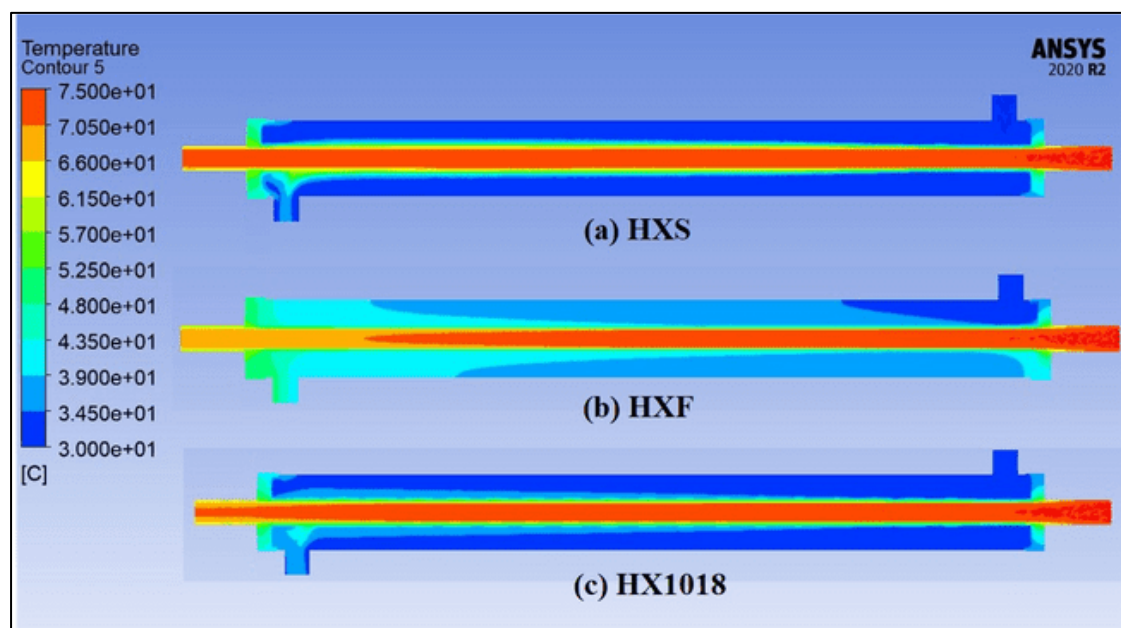


Figure 13 Contour of temperature for a three heat exchangers (front view).

## 5. CONCLUSIONS

A numerical study on the effect of metal foam's volume and pore density in a double pipe heat exchanger has been conducted. A number of heat exchangers of different configurations has been analysed. These configurations are used to cover the performance analysis of heat exchangers performance in the case of smooth pipe, fully filled pipe with copper foam, and partially filled pipe with baffels that have variable thickness and numbers. For all these configurations that uses copper foam, pore density was changed as (10, 20, 30, 40, and 50PPI). After presenting and discussing the obtained results, the following conclusions are made:

- 1- Improvement the average heat transfer rate when added metal foam to a double pipe heat exchangers, and this percentage in an HX1018 was 87.2% (i.e. 1151.4W), while average heat transfer rate in a HXS was (615W).
- 2- Both thermal and hydraulic performance increased when pore density increased, where the average heat transfer rate reached to (17%) at pore density (10-50PPI) in (HXF).
- 3- When the pore density increases, the pressure drop increases in a greater rate than The average Nussle number ( $Nu_{ave}$ ) does which leads to the decrease in performance evaluate criteria (PEC).
- 4- For the same configuration, when the metal foam volume decreases, both thermal and hydraulic performance decrease which consequently lead to the decrease of performance evaluate criteria (PEC).
- 5- Hydraulic performance didnt affected by different distribution of CFB with constant volume of the copper foam.
- 6- Thermal performance is effected by distribution of CFB with a constant volume of copper foam, therefore performance evaluate criteria (PEC) of the HX1018 bigger than the HX209.

To explain the previos, the large surface area of the copper foam led to an increase in the heat transfer rate with the water. This large area results from converting solid metals into porous metals (open-cell metal foam) that contain a voes (open cells) that are connected on its sides. The formation of this porous material and its distribution within the heat exchanger can improve the thermal performance and maintain a low pressure drop without increasing the size of the porous material.

## REFERENCES

- [1] G. B. Abadi and K. C. Kim, "Experimental heat transfer and pressure drop in a metal-foam-filled tube heat exchanger," *Experimental Thermal and Fluid Science*, vol. 82, pp. 42–49, 2017.
- [2] Z. G. Xu, J. Qin, X. Zhou, and H. J. Xu, "Forced convective heat transfer of tubes sintered with partially-filled gradient metal foams (GMFs) considering local thermal non-equilibrium effect," *Applied Thermal Engineering*, vol. 137, pp. 101–111, 2018.
- [3] A. Jamarani, M. Maerefat, N. F. Jouybari, and M. E. Nimvari, "Thermal performance evaluation of a double-tube heat exchanger partially filled with porous media under turbulent flow regime," *Transport in Porous Media*, vol. 120, no. 3, pp. 449–471, 2017.
- [4] T. Fiedler, R. Moore, and N. Movahedi, "Manufacturing and Characterization of Tube-Filled ZA27 Metal Foam Heat Exchangers," *Metals*, vol. 11, no. 8, p. 1277, 2021.
- [5] P. K. Tamkhade, R. D. Lande, R. B. Gurav, and M. M. Lele, "Investigations on tube in tube metal foam heat exchanger," *Materials Today: Proceedings*, vol. 72, pp. 951–957, 2023, doi: 10.1016/j.matpr.2022.09.097.
- [6] Z. Li, A. Shahsavari, A. A. A. Al-Rashed, and P. Talebizadehsardari, "Effect of porous medium and nanoparticles presences in a counter-current triple-tube composite porous/nano-PCM system," *Applied Thermal Engineering*, vol. 167, p. 114777, 2020.
- [7] T. Chen, G. Shu, H. Tian, T. Zhao, H. Zhang, and Z. Zhang, "Performance evaluation of metal-foam baffle exhaust heat exchanger for waste heat recovery," *Applied energy*, vol. 266, p. 114875, 2020.
- [8] F. Zhou, T. Lu, D. Zhuang, and G. Ding, "Experimental study of condensation heat transfer characteristics on metal foam wrapped tubes under sloshing conditions," *International Journal of Heat and Mass*

*Transfer*, vol. 176, p. 121394, 2021.

- [9] A. Niameh and M. Alhusseney, "HEAT TRANSFER ENHANCEMENT USING ROTATING POROUS MEDIA Table of Contents," no. May. University of Manchester, p. 233, 2016.
- [10] H. Abdullah, A. J. Jubear, and H. R. Al-Bugharbee, "Numerical and experimental thermal performance of forced convection in metal foam heat sinks," *International Journal of Mechanical Engineering*, vol. 7, no. 1, pp. 974–5823, 2022.
- [11] E. Ozden and I. Tari, "Shell side CFD analysis of a small shell-and-tube heat exchanger," *Energy Conversion and Management*, vol. 51, no. 5, pp. 1004–1014, 2010.
- [12] H. E. Ahmed, O. T. Fadhil, and T. H. Farhana, "Performance of a double-pipe heat exchanger with different metal foam arrangements," *Anbar Journal of Engineering Sciences*, vol. 12, no. 2, 2021.
- [13] J. A. Hamzah and M. A. Nima, "Experimental study of heat transfer enhancement in double-pipe heat exchanger integrated with metal foam fins," *Arabian Journal for Science and Engineering*, vol. 45, no. 7, pp. 5153–5167, 2020.